Available online at www.sciencedirect.com
SCIENCE DIRECT®
Sedimentary Geology 166 (2004) 353–366
Sedimentary Geology
www.elsevier.com/locate/sedgeo

Factors controlling tufa deposition in natural waters at waterfall sites

Jingan Chen[a,*], David Dian Zhang[b], Shijie Wang[a], Tangfu Xiao[a], Ronggui Huang[a]

[a] State Key Laboratory of Environmental Geochemistry, Institute of Geochemistry, Chinese Academy of Sciences, 46 Guanshui Road, Guiyang 550002, China
[b] Department of Geography and Geology, University of Hong Kong, Pokfulam Road, Hong Kong, China

Received 30 July 2003; received in revised form 19 January 2004; accepted 3 February 2004

Abstract

Study on calcite precipitation has major implications for both the hydrochemical evolutions of river systems and the global carbon cycle. The precipitation of calcite generally requires the water to be 5–10 times supersaturated with respect to calcite, which is usually achieved by the removal of CO_2. Formation of waterfall tufa has been often simply described as the result of water turbulence in fast-flowing water. In this paper, the formation mechanisms of waterfall tufa are discussed and a series of laboratory experiments are designed to simulate the hydrological conditions at waterfall sites. The influences of the air–water interface, the water flow velocity and the solid–water interface on CO_2 outgassing and calcite precipitation are compared and evaluated quantitatively. The results show that the principal cause of waterfall tufa formation is the enhanced inorganic carbon dioxide outgassing resulted from the sudden hydrological changes occurring at waterfall sites, rather than organisms, evaporation or the solid–water interface. The air–water interface area and the water flow velocity are greatly increased at waterfall sites as a result of the "aeration effect", "low pressure effect" and "jet-flow effect", which greatly accelerate CO_2 outgassing. Inorganic CO_2 outgassing drives the waters to become highly supersaturated with respect to calcite and, consequently, results in much calcite deposition. The solid–water interface is less important as the air–water interface in affecting calcite precipitation at waterfall sites. Field measurements showed that conductivity, Ca^{2+} and HCO_3^- concentrations along Tianhe Creek and Hot Creek decrease downstream while pH rises. Field observations also showed that tufa deposition occurred mainly at waterfall sites.

Keywords: Waterfall tufa; CO_2 outgassing; Air–water interface; Flow velocity; Solid–water interface

1. Introduction

The term "tufa" is commonly used for porous, cool, freshwater $CaCO_3$ deposits (Ford and Pedly, 1996; Zhang et al., 2001). Waterfall tufa, which is the calcite deposition that forms at waterfall and cascade sites along river channels, is widely distributed around the world, especially in tropical and subtropical karst regions. Precipitation of calcite in natural water can be simply shown by the following reaction:

$$Ca^{2+} + 2HCO_3^- \Leftrightarrow CaCO_3 \downarrow + CO_2 \uparrow + H_2O \qquad (1)$$

* Corresponding author. Fax: +86-851-5895707.
E-mail address: jinganchen@hotmail.com (J. Chen).

0037-0738/$ - see front matter © 2004 Elsevier B.V. All rights reserved.
doi:10.1016/j.sedgeo.2004.02.003

Calcite precipitation has important influence on both the hydrochemical evolution of river systems and the global carbon cycle because a large amount of CO_2 is released from the water to the atmosphere during the precipitation processes. Generally, precipitation of calcite requires the waters to be 5–10 times supersaturated with respect to calcite because of lack of free energy to create new surface areas, unavailability of reactive calcite to act as nucleation sites, and inhibition of PO_4^{3-}, Mg^{2+} and organic ligands (Berner, 1975; Reddy, 1977; Dandurand et al., 1982; Buhmann and Dreybrodt, 1987; Lorah and Herman, 1988; Lebron and Suarez, 1996). This is why river water is generally supersaturated with respect to calcite but calcite precipitation does not occur along the entire river channel. In the Colorado River system of the southwest United States, calcite precipitation is not detectable although the water reaches four to six times supersaturation with respect to calcite (Suarez, 1983).

The mechanisms of tufa formation have been investigated by many scientists since the 1980s. It is well known that high supersaturation of water with respect to calcite usually results from the removal of CO_2 from the water. Several studies have attributed the CO_2 removal to turbulence, mixing of different waters and metabolic uptake of CO_2 by photosynthetic plants (Jacobson and Usdowski, 1975; Chafetz and Folk, 1984; Herman and Lorah, 1987; Viles and Goudie, 1990). Chafetz and Folk (1984) present convincing evidence that bacterially precipitated calcite forms a large percentage of tufa accumulations in Italy and the USA. Viles and Goudie (1990) and Janssen et al. (1999) also noted tufa formation is commonly associated with organisms. However, studies of waterfall tufa have shown that a great amount of inorganic CO_2 outgassing occurs at waterfall sites (Zhang and Mo, 1982; Chafetz and Folk, 1984; Lorah and Herman, 1988; Ford, 1989; Zhang et al., 2001; Drysdale et al., 2002). Through detailed field measurements of temperature, pH, calcium concentration and alkalinity in two small streams in southwest Germany, Merz-Preiß and Riding (1999) found that the principal cause of supersaturation in fast-flowing streams is inorganic carbon dioxide outgassing while photosynthetic uptake of carbon dioxide and temperature effects are negligible. It seems that organisms play an insignificant role in waterfall tufa formation although they may indirectly aid in tufa formation by trapping microparticle and providing a substrate for calcite growth. This is testified by the field observation that organisms exist along the entire river channel, but tufa deposition occurs mainly at waterfall site. However, development of waterfall tufa has been simply described as the result of water turbulence. Knowledge about how environmental conditions change at waterfall sites and how these changes affect calcite precipitation is rather scarce. We believe the principal cause of waterfall tufa formation is the sudden hydrological changes occurring at waterfall sites. In this paper, a series of experiments are designed to simulate the hydrological changes at waterfall sites, and the influences of various factors on calcite precipitation are evaluated quantitatively.

2. Research design and experiments

Understanding the hydrological changes occurring at waterfall sites is the key to design simulating experiments and to thus investigate the factors controlling tufa formation. Three major changes occur when river channel flow approaches a waterfall. Firstly, the sudden changes in flow conditions at waterfall sites can lead to air entrainment, which are termed "natural aeration" (Kobus, 1991). In rivers, aeration can appear in high-velocity flow, plunging free-jet flow, the wakes of topographic irregularities on channel beds, and in hydraulic-jump configurations, which suck and trap air inside the water body and create many air bubbles (Chanson and Qiao, 1994; Chanson and Cummings, 1996; Chanson and Toombes, 2003). These conditions are most obvious at waterfall sites, where "white-water phenomena" occurs. Here we call the phenomena induced by air entrainment as "aeration effect".

Secondly, water pressure at high velocity at waterfall sites is reduced according to the Bernoulli effect (described in Section 3). At lower pressures, dissolved gases can be released from water as tiny air bubbles according to the Henry's law. This results in air detrainment at waterfall sites and is called "low pressure effect".

Finally, the fast-flowing and falling water at waterfall sites is broken into many water droplets, small

streams and sprays due to the initial jet-flow turbulence and to the shear forces of the surrounding air. We call this phenomenon "jet-flow effect".

The "aeration effect" creates air bubbles at waterfall sites that can greatly increase the size of the air–water interface area. The "low pressure effect" at high flow velocity not only creates bubbles and thus enlarges the air–water interface area, but also reduces CO_2 content in the water resulting from detraining of the dissolved gases from the water flow. The "jet-flow effect" usually results in much larger air–water interface area because the jet flows consist of sprays, droplets and broken streams (Chanson and Cummings, 1996; Zhang et al., 2001). Thus, it can be seen the main hydrological changes, occurring at waterfall sites as a result of these effects, are the enlargement of the air–water interface area and the increase of the flow velocity of the water. We believe these two hydrological changes are the major cause of waterfall tufa deposition. In order to testify our hypothesis, a series of laboratory experiments were designed to simulate the changes of the air–water interface area and the flow condition at waterfall sites, and to evaluate quantitatively their influences on CO_2 outgassing and calcite precipitation. Field measurements in two creeks were carried out in order to improve our understanding of CO_2 outgassing and calcite precipitation in natural river waters.

In order to acquire quantitative data on calcite precipitation rates, we need to continuously monitor the Ca^{2+} concentration changes. In fact, it is impossible to determine Ca^{2+} concentration continuously and accurately during the simulating processes because it will change the simulating conditions and thus affect the simulating results when a part of solution is taken out for Ca^{2+} concentration determination by the Atomic Absorption Spectrometer (AAS). Fortunately, conductivity, which along carbonate-depositing systems fluctuates primarily as a result of carbonate depositions (Drysdale et al., 2002), is often a good tracer of Ca^{2+} concentration changes in natural karst water (Groleau et al., 2000; Drysdale et al., 2002). In order to testify whether conductivity variability can represent Ca^{2+} concentration changes, Ca^{2+} concentrations and conductivities of laboratory solutions with different Ca^{2+} concentrations were measured respectively by the Atomic Absorption Spectrometer (PE5100) and the Portable Multi-parameter Instrument (pIONneer 65). The good correlation between them (Fig. 1) suggests that conductivity can be used as a surrogate measure of Ca^{2+} concentration. Ca^{2+} concentrations can be calculated according to the initial Ca^{2+} concentration and the conductivity in the waters. Furthermore, calcite precipitation rate can be deduced from the Ca^{2+} concentration changes.

$CaCO_3$ solution for simulating experiments was prepared by adding pure $CaCO_3$ grains in a 10-l glass container full of distilled water. Pure CO_2 gas was then continuously pumped into the water for 72 h. The $CaCO_3$ solution was passed through a 0.45-μm filter before using as sample solutions for experimental studies. The initial conductivities of the sample waters ranged from 1050 to 1210 μs.

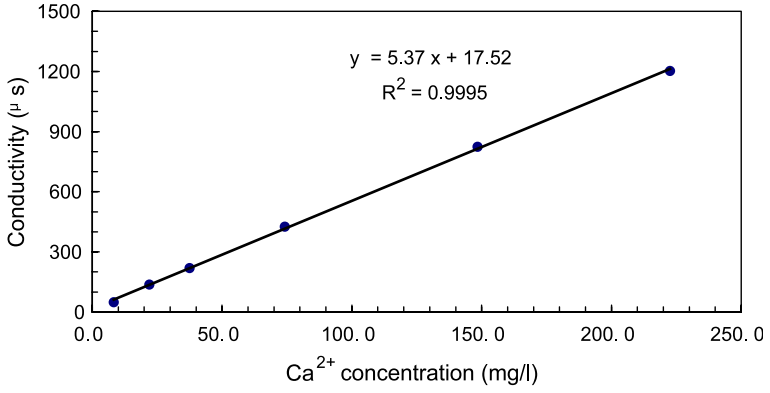

Fig. 1. The correlation between Ca^{2+} concentration and conductivity in sample waters.

All the following simulating experiments were carried out in a cultivator box set to 20 °C in order to eliminate the influence of the temperature on calcite precipitation. Changes of conductivity and pH in sample waters were measured respectively by the Portable Multi-parameter Instrument (pIONneer 65) and by an Orion 818 pH meter. The pH electrode was calibrated with pH 4.00 and 6.86 buffers every 2 h.

2.1. Calcite precipitation processes experiment

The first aim of this experiment is to systematically comprehend the calcite precipitation processes and the second aim is to examine the dependence of calcite precipitation on CO_2 outgassing. The 550-ml sample solution was put into a 11.21-cm diameter cylindrical glass vessel with a water-surface area of 98.70 cm^2. The pH and conductivity of the sample solution were measured under stationary condition at time intervals of 10–20 min at the beginning in order to understand the fast-changing process, and at time intervals of 30–60 min when the sample solution showed only small fluctuations in pH and conductivity and finally appeared to reach equilibrium.

The ''equilibrated'' solution was filtered through a 0.45-μm filter, and its Ca^{2+} concentration was measured by the Atomic Absorption Spectrometer (PE5100) in order to calculate calcite precipitation rate.

2.2. Air–water interface experiments

In order to evaluate quantitatively the influence of air–water interface on calcite precipitation, 550-ml sample solutions were respectively put into three cylindrical glass vessels with different water-surface areas of 55.65, 98.70 and 155.49 cm^2. These sample solutions had the same initial conductivity of 1052 μs. Conductivity changes with time in the three sample waters were measured by the Portable Multi-parameter Instrument (pIONneer 65) under stationary condition at time intervals of about 10 h until the solutions appeared to stop precipitating. Ca^{2+} concentrations of the initial solutions and the ''equilibrated'' solutions were measured by the Atomic Absorption Spectrometer (PE5100) after they were filtered through a 0.45-μm filter.

2.3. Flowing water experiments

The first aim of this experiment is to evaluate quantitatively the influence of the water flow velocity on calcite precipitation, with the second aim comparing the calcite precipitation rates in standing and flowing waters. The 550-ml sample solution with an initial conductivity of 1031 μs was put into a cylindrical glass vessel with a water-surface area of 55.65 cm^2. The glass vessel was put on a magnetic beater and a round magnetic rod with a length of 4 cm was put in the middle of the bottom of the vessel in order to bring the solution to move. When the magnetic beater worked, the sample solution had a rotation rate of 30 rps (i.e. an average flow velocity of 4 m/s). Conductivity changes were measured under flowing condition at time intervals of 10–20 min at the beginning and at time intervals of 30–60 min when the sample solution showed only small conductivity fluctuations and gradually approached equilibrium. As a comparison, 550-ml sample solution with an initial conductivity of 1049 μs was put into a cylindrical glass vessel with the same water-surface area of 55.65 cm^2, and conductivity changes under stationary condition were monitored every 10–20 min at the beginning and every 30–60 min when the solution showed only small conductivity fluctuations.

2.4. Solid–water interface experiments

In order to evaluate quantitatively the influence of the solid–water interface on calcite precipitation and examine the relative importance of the air–water interface and the solid–water interface, 550-ml water samples were respectively put into two cylindrical glass vessels with the same surface area of 55.65 cm^2, one of which a calcite tablet with a surface area of 65.31 cm^2 was put in the middle of the bottom. The sample solutions had the same initial conductivity of 1180 μs. Conductivity changes in these two solutions were monitored by the Portable Multi-parameter Instrument (pIONneer 65) under stationary condition at time intervals of about 10 h until the solutions appeared to stop

precipitating. Ca^{2+} concentrations of the initial solutions and the "equilibrated" solutions were measured by the Atomic Absorption Spectrometer (PE5100) after they were filtered through a 0.45-μm filter in order to compare their calcite precipitation rates.

2.5. Field measurement of river waters

With an aim of improving our understanding of CO_2 outgassing and calcite precipitation in natural river waters, field measurements were carried out along Tianhe Creek and Hot Creek, which are located in Guizhou Province, a typical Karst region in Southwest China. The two creeks typically are less than 40 cm in depth and 3 m or less in width. There is no obvious resurgence of groundwater downstream. Six sites were respectively selected and examined in each of the two creeks. Sites were not evenly spaced, but located to monitor hydrochemical changes at waterfall sites and cascades (Fig. 2). All sample were sampled within 2 h in order to eliminate the influences of diurnal changes of hydrochemical parameters on the interpretation of downstream changes (Drysdale et al., 2002). Conductivity and pH in river waters were measured respectively by the Portable Multi-parameter Instrument (pIONneer 65) and by the Orion 818 pH meter. Standard HCl titration method was applied to measure HCO_3^- concentrations after the waters were filtrated in field. Upon return to the laboratory, the waters were passed through a 0.45-μm filter and Ca^{2+} concentrations were determined by the Atomic Absorption Spectrometer (PE5100).

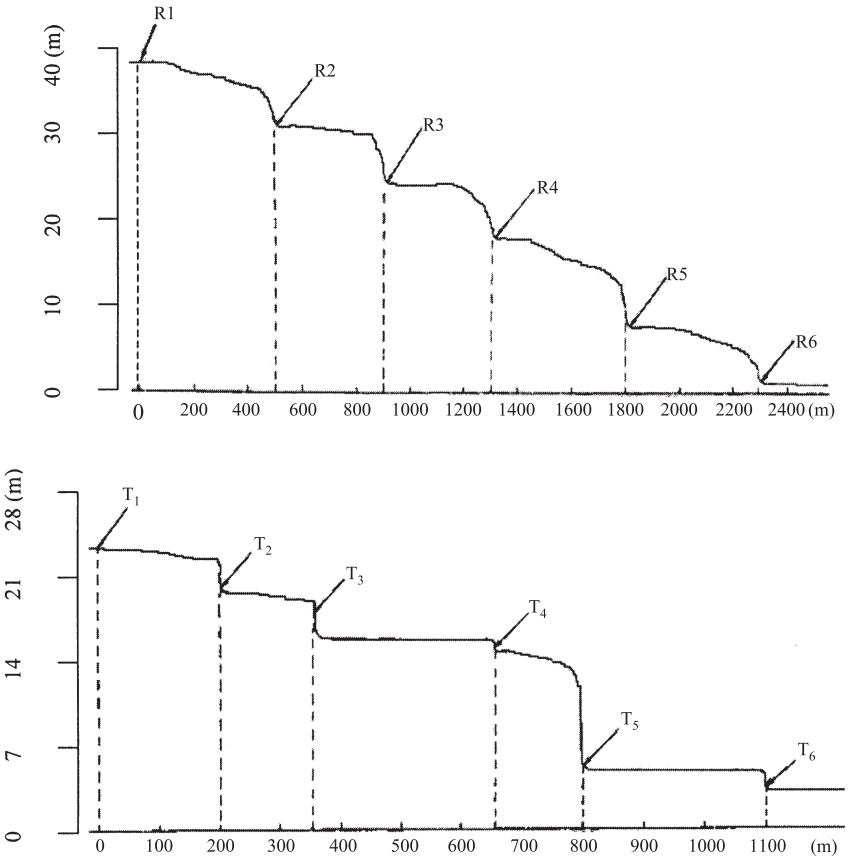

Fig. 2. Sample localities sketch map along Hot Creek (R1–R6) and Tianhe Creek (T1–T6).

All the measurements were completed within 24 h of sampling.

3. Results

3.1. Calcite precipitation processes observed under stationary condition

The pH and conductivity changes with time under stationary condition were shown in Fig. 3, from which the following three stages can be identified.

3.1.1. The fast degassing stage

This stage lasted about 25 h and was characterized by the constant conductivity and the rapid increase in pH (Fig. 3). The P_{CO_2} difference between the ambient atmosphere and the sample water resulted in quick diffusion of CO_2 from the water to the atmosphere, and thus led to the reduction in H^+ content. This process can be shown by Eq. (2).

$$H^+ + HCO_3^- \Leftrightarrow H_2CO_3 \Leftrightarrow CO_2\uparrow + H_2O \quad (2)$$

The water's supersaturation degree with respect to calcite is usually expressed by IAP/K_e where IAP represents the ionic activity product and K_e represents the equilibrium constant of $CaCO_3$. One convenient method for the computation of IAP is:

$$\begin{aligned} IAP &= (Ca^{2+})(CO_3^{2-}) \\ &= \{r_{Ca^{2+}} \times [Ca^{2+}] \times r_{HCO_3^-} \times K_2 \times Alk\}/(H^+) \end{aligned} \quad (3)$$

Where r_{Ca}^{2+} and $r_{HCO_3}^-$ are respectively the activity coefficients of Ca^{2+} and HCO_3^-, $[Ca^{2+}]$ is the Ca^{2+} concentration, K_2 is the second dissociation constant for H_2CO_3, Alk is the alkalinity of the water, (H^+) is the H^+ activity defined through measuring pH values ($pH = -\log(H^+)$). From Eq. (3), it can be easily seen that the water's supersaturation degree with respect to calcite increases with the reduction in H^+ content. Detailed calculations showed the sample water's supersaturation degree with respect to calcite increases from 0.82 to 6.97 when pH rises from 6.22 at the beginning to 7.15 at the end of this stage. However, the constant conductivity of the sample water indicated calcite precipitation did not commence. The calcite precipitation rate is almost equal to zero during this stage (Fig. 3).

3.1.2. The fast precipitation stage

This stage lasted about 170 h and was characterized by sharp drop in conductivity (Fig. 3), which reflected the rapid precipitation of calcite. Because of the great loss of CO_2 during the fast degassing stage, the water's supersaturation degree with respect to

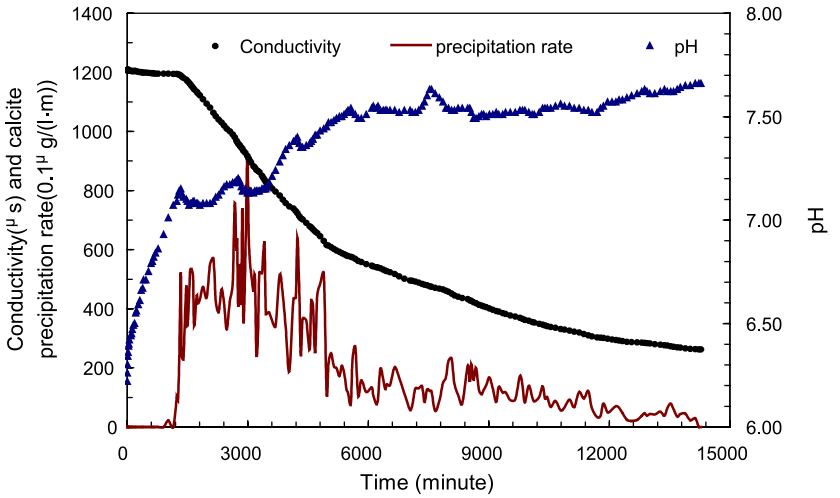

Fig. 3. Changes of conductivity, pH and calcite precipitation rate in the sample water under stationary condition.

calcite rose to so high a level that the nucleation barrier can be overcome and the fast calcite precipitation started. Much H^+ was released to the solution during the processes of the calcite precipitation, leading to the decrease of pH, which can be shown by the Eq. (4). On the other hand, the released H^+ and HCO_3^- gradually converses into CO_2 (Dreybrodt et al., 1997), leading to the reduction in H^+ content, which can be shown by the reaction (5). When the consumption of H^+ was balanced by its production, the pH value remained stable. When the consumption rate of H^+ outpaced its production rate, the pH value rose. When the conversion rate slowed down, the pH value again declined. These processes handed over to substitute the emergence during the whole stage and led to the frequent fluctuations of pH (Fig. 3). The calcite precipitation rates ranged from 8.0 to 92.0 μg/(l m) during this stage with an average of 27.6 μg/(l m) (Fig. 3).

$$Ca^{2+} + 2HCO_3^- \Leftrightarrow CaCO_3 \downarrow + HCO_3^- + H^+. \quad (4)$$

$$H^+ + HCO_3^- \Leftrightarrow CO_2 \uparrow + H_2O \quad (5)$$

3.1.3. The equilibrium stage

This stage is characterized by the relatively stable conductivity and pH value (Fig. 3). The rates of CO_2 outgassing and calcite precipitation slowed down because the P_{CO_2} difference between the atmosphere and the sample water gradually decreased and the solution gradually approached "equilibrium". The calcite precipitation rates were below 8.0 μg/(l m) with an average of 4.2 μg/(l m) (Fig. 3).

Although the conductivity of the sample solution decreased with the time, the calcite precipitation rates fluctuated from time to time (Fig. 3). Two reasons may contributed to this phenomenon. Firstly, the sample solution was supersaturated with respect to calcite, so the conductivity showed a decreasing trend during the calcite precipitation processes. Secondly, the water's supersaturation degree with respect to calcite changed as a result of the frequent pH fluctuations (Fig. 3) according to Eq. (3), causing the calcite precipitation rates to vary from time to time.

3.2. The influence of the air–water interface on calcite precipitation

Conductivity variations under stationary condition in the three sample solutions respectively with water-surface areas of 55.65, 98.70 and 155.49 cm^2 were shown in Fig. 4.

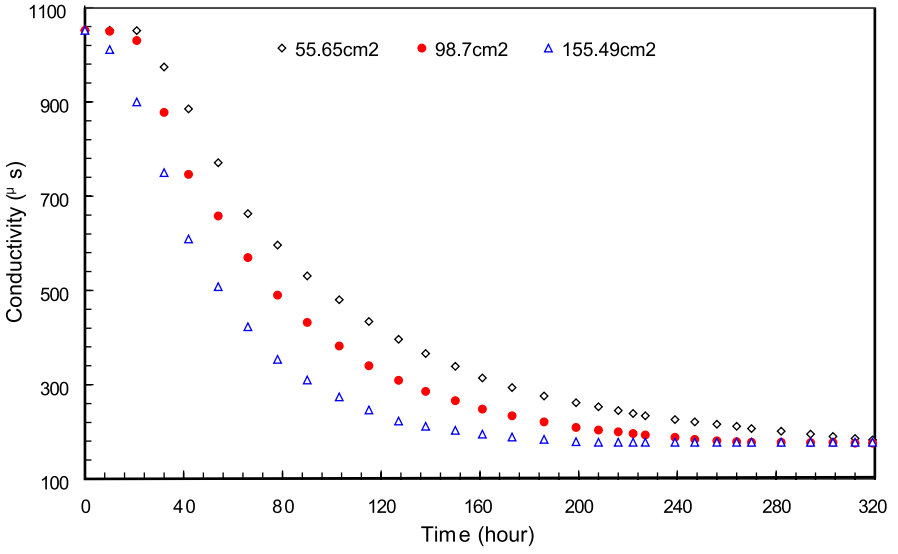

Fig. 4. Conductivity evolution in sample solutions with different surface areas.

Table 1
Comparison of calcite precipitation rates in solutions with different interface areas

Surface area (cm^2)	Initial Ca^{2+} concentration (mg/l)	Equilibrated Ca^{2+} concentration (mg/l)	Equilibrium time (h)	Precipitation rate (mg/l·h)
55.65	254.6	38.8	312	0.69
98.70	254.6	38.4	247	0.88
155.49	254.6	37.9	173	1.25

Obviously, an enlargement of air–water interface area not only accelerated calcite precipitation indicated by faster decrease of conductivity (Fig. 4), but also shortened the period for the sample water to reach the equilibrium (Table 1). The high correlation coefficient between the size of the air–water interface area and the calcite precipitation rate (Fig. 5) suggests that the calcite precipitation rate, to a great extent, depends on the size of the air–water interface area. Higher P_{CO_2} in the water than in the ambient atmosphere drive CO_2 to diffuse quickly from the water to the air. All other things being equal; the larger the air–water interface area is, the faster CO_2 diffuses, the earlier the calcite precipitation commences. In fact, this phenomenon can be well explained by the diffusion theory. The mass transfer rate of a chemical across an interface is a function of the molecular diffusion coefficient, the negative gradient of gas concentration and the interface area. If the chemical of interest is volatile (e.g. CO_2), the gas transfer rate may be expressed as:

$$\frac{d}{dt}C_{gas} = K_L \times \alpha \times (C_{sat} - C_{gas}) \quad (6)$$

where C_{gas} is the dissolved gas concentration, K_L is the mass transfer coefficient, α is the specific surface area and C_{sat} is the concentration of the dissolved gas in water at equilibrium (Gullier, 1990; Chanson, 1995; Chanson and Toombes, 2003). The mass transfer coefficient (K_L) is almost constant (Kawase and Moo-Yong, 1992). The specific surface area (α) is defined as the air–water surface area per unit volume of air and water (Chanson, 1995; Chanson and Toombes, 2003). In our experiments, the three sample solutions have the same volume, the same C_{sat} and the same initial C_{gas}, so the variations of the specific surface area can be represented by the changes of the air–water interface area, and the Eq. (6) can be simplified as:

$$\frac{d}{dt}C_{gas} = K \times S \times (C_{sat} - C_{gas}) \quad (7)$$

where K is a constant and S is the air–water interface area. It is obvious from Eq. (7) that the sizes of the air–water interface area decide the CO_2 outgassing rate and thus control the calcite precipitation rate. This may explain the reason of the high correlation coefficient between the size of the air–water interface area and the calcite precipitation rate in our experiments (Fig. 5).

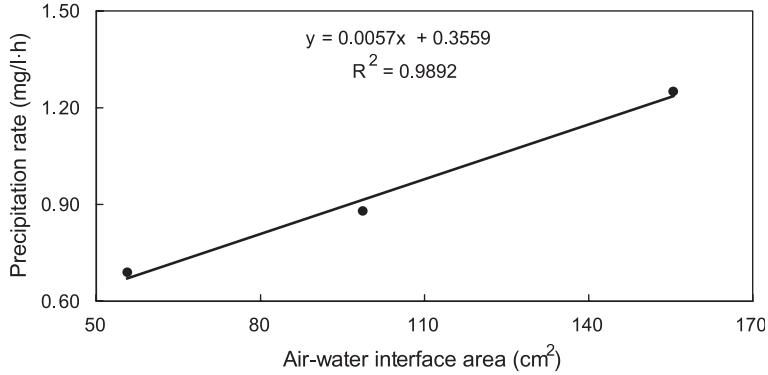

Fig. 5. Correlation between the size of the air–water interface area and the calcite precipitation rate.

Merz-Preiß and Riding (1999) found the greater channel width (i.e. larger air–water interface area) allowed more rapid CO_2 outgassing while the narrower channel limited CO_2 outgassing and calcite precipitation. This provided direct field evidence for our experiment results.

3.3. The influence of the flow velocity on calcite precipitation

Conductivity changes in sample waters under stationary condition and under flowing condition are shown in Fig. 6.

From Fig. 6 and Table 2, it can be seen that the calcite precipitation rate in flowing water is more than four times larger than in stationary water, while the equilibrium time is only one fourth of that in stationary water. This gives clear evidence for the influence of flowing conditions on calcite precipitation rates.

The behavior of a fluid under varying flow conditions is described quantitatively by Bernoulli's law:

$$P + \frac{1}{2}\rho v^2 + \rho g h = [\text{constant}], \quad (8)$$

where P is the static pressure (N/m^2), ρ is the fluid density (kg/m^3), v is the velocity of fluid flow (m/s) and h is the height above a reference surface (m). The effect described by this law is called the Bernoulli effect. Obviously, an increase in the velocity of flow will result in a decrease in the static pressure from Eq. (8), so the water pressure is lower in a moving fluid than in a stationary fluid.

Table 2
Calcite precipitation rates in sample waters under stationary and flowing conditions

Flow condition	Initial Ca^{2+} concentration (mg/l)	Equilibrated Ca^{2+} concentration (mg/l)	Equilibrium time (h)	Precipitation rate (mg/l·h)
Stationary	254.6	38.8	312	0.69
Flowing	251.7	38.1	70	3.05

It is well known that the solubility of a gas in water decreases with decreasing pressure if the temperature stays constant according to the Henry's law, which states

$$P = kC \quad (9)$$

Where P is the static pressure (N/m^2), C is the gas concentration and k is the Henry's law constant, which is the same for the same tem-

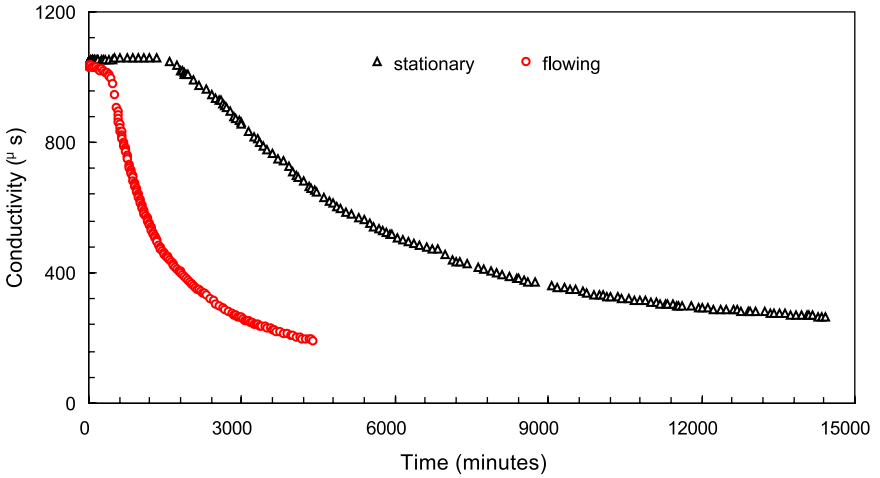

Fig. 6. Conductivity changes with time under stationary and flowing conditions.

perature, gas and solvent. From Eqs. (8) and (9), we can get

$$C = ([\text{constant}] - \rho gh - \rho v^2/2)/k \quad (10)$$

Obviously, the solubility of a gas in water decreases with increasing flow velocity according to Eq. (10). Therefore, dissolved gases can diffuse more quickly from flowing water than from stationary water. On the other hand, fast flowing water not only induces turbulence which can cause more effective collision between dissolved ions and therefore accelerate chemical reactions, but also reduces the thickness of diffusion boundary layers in both solid–water and air–water interface, which accelerates the mass transfer through the two interfaces and thus increases calcite deposition rate (Bogli, 1980; Liu et al., 1995). All these factors together caused much earlier and faster calcite precipitation in flowing water than in stationary water. This phenomenon also occurs in field. Liu et al. carried out in situ experiments to measure calcite deposition rates at the dam sites with fast water flow (0.5–2 m/s) as well as inside pools with still water in Huanglong Ravine, China. The result showed that depositional rates in fast flowing water were higher by as much as a factor of four compared to still water although there were no differences in hydrochemistry (Liu et al., 1995). The good agreement between the field measurements and our laboratory observations provide convincing evidence that the flowing conditions exert a large influence on calcite precipitation rates in natural waters.

3.4. Calcite precipitation in waters with different solid–water interface areas

Although an increase of solid–water interface area accelerated the calcite precipitation (Fig. 7), but it did not affect the precipitation rate as much as an increase of air–water interface area (Fig. 4). Moreover, when river water flows over a waterfall, there is much greater increase of the air–water interface area than that of the solid–water interface area. Therefore, the air–water interface is much more important in controlling calcite precipitation than the solid–water interface at waterfall sites. CO_2 outgassing plays a major role in causing calcite precipitation.

3.5. Chemical evolution in two natural rivers

The field measurements showed that patterns of downstream variations in pH, conductivity, Ca^{2+} concentrations and HCO_3^- concentrations are generally comparable in these two creeks (Fig. 8). Conductivity, Ca^{2+} concentrations and HCO_3^- concentrations decreased downstream along the river channels (Table 3 and Fig. 8) while pH rose. This

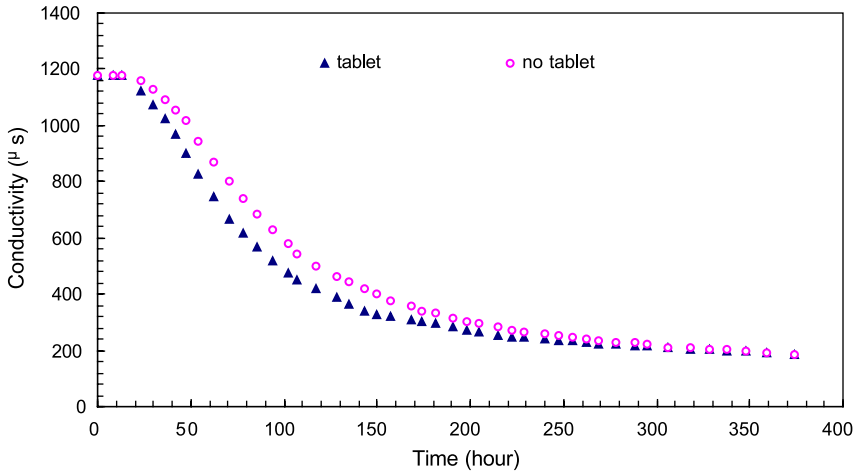

Fig. 7. Conductivity evolution of solutions with/without calcite tablet.

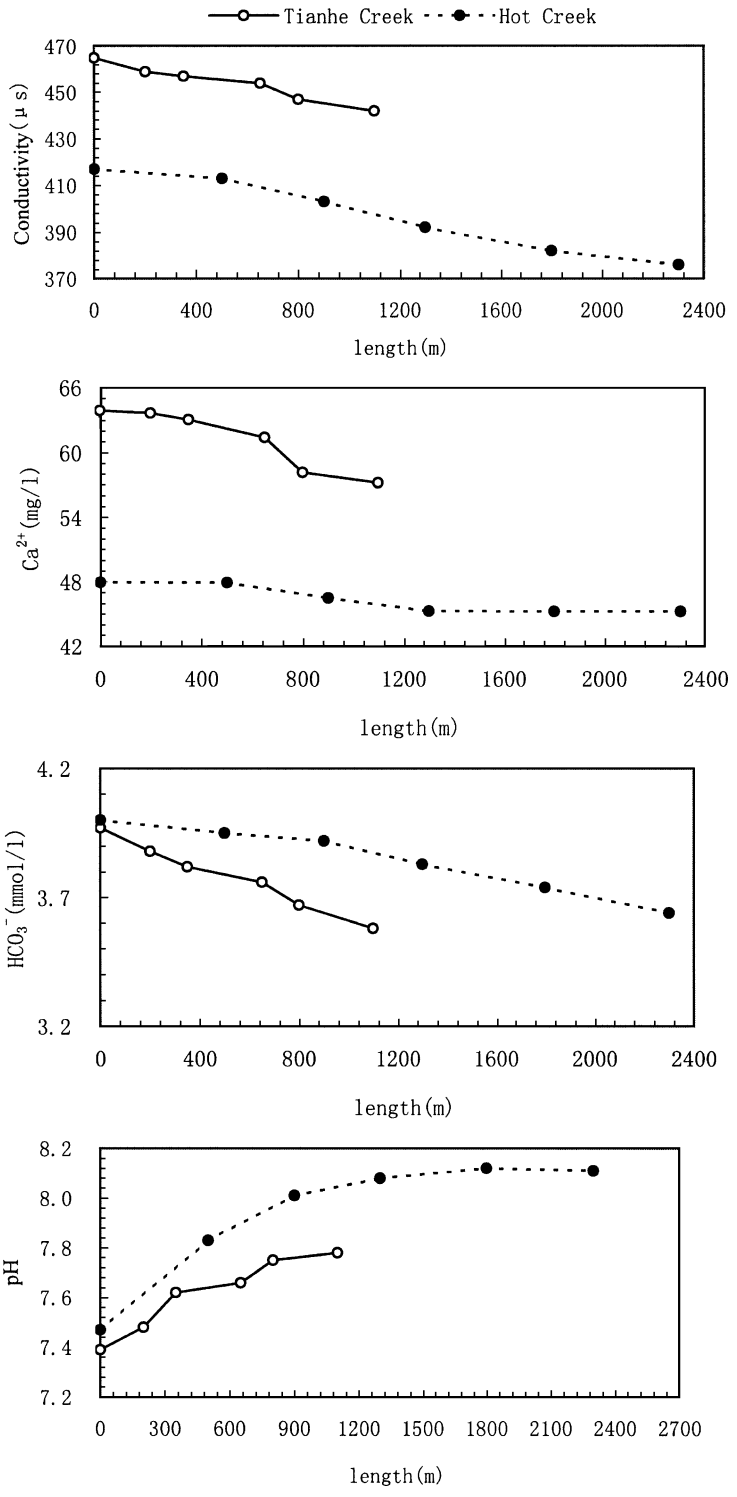

Fig. 8. Downstream changes in the chemical properties of Tianhe Creek and Hot Creek.

Table 3
Hydrochemical evolution along Tianhe Creek and Hot Creek

Tianhe Creek					Hot Creek				
Length (m)	Ca^{2+} (mg/l)	Conductivity (μs)	pH	HCO_3^- (mg/l)	Length (m)	Ca^{2+} (mg/l)	Conductivity (μs)	pH	HCO_3^- (mg/l)
0	63.91	465	7.39	242.23	0	47.96	417	7.47	243.92
200	63.66	459	7.48	236.60	500	47.94	413	7.83	241.11
350	63.04	457	7.62	233.22	900	46.48	403	8.01	238.85
650	61.39	454	7.66	229.28	1300	45.26	392	8.08	233.78
800	58.15	447	7.75	223.64	1800	45.24	382	8.12	228.15
1100	57.21	442	7.78	218.57	2300	45.24	376	8.11	221.95

reflected the processes of CO_2 outgassing and calcite precipitation downstream. The highest waterfalls and cascades generally have the most obvious decreases of conductivity, Ca^{2+} and HCO_3^- concentrations. Field observations also showed that tufa deposition occurred mainly at waterfall sites.

4. Discussions and conclusions

Until now, several factors have been found to attribute to tufa formation.

4.1. Organisms

The effects of organisms (such as plants, algae, bacteria, cyanobacteria, diatoms and mosses) on tufa formation can be divided into physical effects and chemical effects. The physical effects are encrustation, trapping and binding, assimilation, nucleation and secretion (Chafetz and Folk, 1984; Emeis et al., 1987; Pentecost and Lord, 1988; Viles and Goudie, 1990; Pedley, 1992; Zhang et al., 2001). However, the physical effects cannot result in the waters becoming supersaturated with respect to calcite, which is the prerequisite of calcite precipitation. The chemical effects lie mainly in photosynthesis, which takes up CO_2 from water and causes supersaturation (Kelts and Hsu, 1978; Stumm, 1985; Chen et al., 2002). However, the slowest CO_2 outgassing rate calculated from our experiments and other experiments in the field (Lorah and Herman, 1988; Liu et al., 1995; Lu et al., 2000; Zhang et al., 2001) is at least 10 times greater than the fastest CO_2 uptake rate by algae (Geider and Osborne, 1992), which suggests that CO_2 consumed by organisms is much less than the CO_2 lost by outgassing at waterfall sites. Therefore, organisms cannot be the major cause of tufa formation at waterfall sites although they may play a major role in calcite precipitation where water is quiescent or slowly flowing such as in lake waters when CO_2 outgassing rate is very low. This is supported by the fact that tufa is mainly deposited at waterfall sites although organisms exist along the entire river channel in the investigated rivers.

4.2. Evaporation

Evaporation can reduce water volume and increase the ion concentrations in waters, even directly results in the waters becoming supersaturated with respect to calcite and induces calcite precipitation (Chen et al., 2002). However, this usually occurs when the water experiences long-time strong evaporation, for example in brine lakes. At waterfall sites, the fast-flowing water passes the waterfall usually within several minutes, so the evaporation cannot play major role in calcite precipitation.

4.3. Changes of hydrological conditions

As noted before, the "aeration effect", the "low pressure effect" and the "jet-flow effect" result in two major hydrological changes at waterfall sites. Firstly, the air–water interface area is greatly enlarged. Secondly, the flow velocity of the water increases when river channel flow approaches a waterfall. Our laboratory experiments have proven that larger size of the air–water interface area lead to faster calcite precipitation rate, and the fast-

flowing water can cause much faster calcite precipitation than in stationary water. Therefore, we believe the enlargement of the air–water interface area and the high flow velocity at waterfall sites contribute to the waterfall tufa deposition.

4.4. Solid–water interface

Larger solid–water interface area may result in faster calcite precipitation because more nucleation sites are available, which is helpful for overcoming the kinetic thresholds to calcite precipitation. However, our experiments showed that the solid–water interface did not affect calcite precipitation as much as the air–water interface. Moreover, there is much greater increase of the air–water interface area than that of the solid–water interface area when river water flows over a waterfall. Therefore, the influence of the water–solid interface on calcite precipitation is negligible. Nevertheless, it should be noted that solids at waterfall sites play important role in keeping calcite particles. If there is no direct precipitation on solids, all calcite particles will flow downstream and are lost.

In conclusion, the dominant factors controlling waterfall tufa formation are the hydrological changes instead of organisms, evaporation or the solid–water interface. Inorganic CO_2 outgassing is the principal process driving the waters becoming highly supersaturated with respect to calcite and induces calcite precipitation at waterfall sites. The air–water interface area and the water flow velocity are greatly increased at waterfall sites as a result of the ''aeration effect'', ''low pressure effect'' and ''jet-flow effect'', which greatly accelerates CO_2 outgassing, drive the waters to high levels of calcite supersaturation and consequently results in much calcite deposition. This is the major cause of waterfall tufa formation.

Acknowledgements

This work was supported by the CRCG Seed Grant of the University of Hong Kong and the National Natural Science Foundation of China (No. 90202003). We thank Dr. H. Martyn Pedley and an anonymous reviewer for helpful comments.

References

Berner, R.A., 1975. The role of magnesium in the crystal growth of calcite and aragonite from seawater. Geochimica et Cosmochimica Acta 39, 489–504.

Bogli, A., 1980. Karst Hydrology and Physical Speleology. Springer, Berlin.

Buhmann, D., Dreybrodt, W., 1987. Calcite dissolution kinetics in the system $H_2O–CO_2–CaCO_3$ with participation of foreign ions. Chemical Geology 64, 89–102.

Chafetz, H.S., Folk, R.L., 1984. Travertine: depositional morphology and the bacterially constructed constituents. Journal of Sedimentary Petrology 54, 289–316.

Chanson, H., 1995. Air–water gas transfer at hydraulic jump with partially developed inflow. Water Research 29, 2247–2254.

Chanson, H., Cummings, P.D., 1996. Air–water interface area in supercritical flows down small slope chutes. Department of Civil Engineering Research Series No. CE151, University of Queensland.

Chanson, H., Qiao, G.L., 1994. Air bubble entrainment and gas transfer at hydraulic jump. Department of Civil Engineering Research Series No. CE149, University of Queensland.

Chanson, H., Toombes, L., 2003. Strong interactions between free-surface aeration and turbulence in an open channel flow. Experimental Thermal and Fluid Science 27, 525–535.

Chen, J.A., Wan, G.J., Wang, F.S., Zhang, D.D., Huang, R.G., Zhang, F., Schmidt, R., 2002. Carbon environmental records in recent lake sediments. Science in China, Series D 45, 875–884.

Dandurand, J.L., Gout, R., Hoefs, J., Menschel, G., Schott, J., Usdowski, E., 1982. Kinetically controlled variations of major components and carbon isotopes in a calcite-precipitating spring. Chemical Geology 36, 299–315.

Dreybrodt, W., Elsenlohr, L., Madry, B., Ringer, S., 1997. Precipitation kinetics of calcite in the system $CaCO_3–H_2O–CO_2$: the conversion to CO_2 by the slow process $H^+ + HCO_3^- \rightarrow CO_2 + H_2O$ as a rate limiting step. Geochimica et Cosmochimica Acta 361, 3897–3904.

Drysdale, R.N., Taylor, M.P., Ihlenfeld, C., 2002. Factors controlling the chemical evolution of travertine-depositing rivers of the Barkly karst, northern Australia. Hydrological Processes 16, 2941–2962.

Emeis, K.C., Richnow, H.H., Kempe, S., 1987. Travertine formation in Plitvice National Park: chemical versus biological control. Sedimentology 34, 595–610.

Ford, T.D., 1989. Tufa: a freshwater limestone. Geology Today 5, 60–63.

Ford, T.D., Pedly, H.M., 1996. A review of tufa and travertine deposits in the world. Earth Sciences Reviews 41, 117–175.

Geider, R.J., Osborne, B.A., 1992. Algae Photosynthesis: the Measurement of Algae Gas Exchange. Chapman & Hall, New York.

Groleau, A., Sarazin, G., Vincon-Leite, B., Tassin, B., Quiblier-Lloberas, C., 2000. Tracing calcite precipitation with specific conductance in a hard water alpine lake. Water Research 34, 4151–4160.

Gullier, J.S., 1990. Introduction to air–water mass transfer. In: Wilhelms, J.S., Gullier, J.S. (Eds.), Proceedings of the 2nd In-

ternational Symposium on Gas Transfer at Water Surfaces, Air–Water Mass Transfer. ASCE, Minneapolis, MN, USA, pp. 1–7.

Herman, J.S., Lorah, M.M., 1987. CO_2 outgassing and calcite precipitation in Falling Spring Creek, Virginia, USA. Chemical Geology 62, 251–262.

Jacobson, R.L., Usdowski, E., 1975. Geochemical controls on a calcite precipitating spring. Contributions to Mineralogy and Petrology 51, 65–74.

Janssen, A., Swennen, R., Podoor, N., Keppens, E., 1999. Biological and diagenetic influence in recent and fossil tufa deposits from Belgium. Sedimentary Geology 126, 75–95.

Kawase, Y., Moo-Yong, M., 1992. Correlations for liquid-phase mass transfer coefficients in bubble column reactors with Newtonian and non-Newtonian fluids. Canadian Journal of Chemical Engineering 70, 48–54.

Kelts, K., Hsu, K.J., 1978. Freshwater carbonate sedimentation. In: Lerman, A. (Ed.), Lakes: Chemistry, Geology, Physics. Springer-Verlag, Berlin, pp. 295–323.

Kobus, H., 1991. Introduction to air–water flow. In: Wood, I.R. (Ed.), Air Entrainment in Free-Surface Flows. Balkema, Rotterdam, pp. 1–28.

Lebron, I., Suarez, D.L., 1996. Calcite nucleation and precipitation kinetics as affected by dissolved organic matter at 25 °C and pH>7.5. Geochimica et Cosmochimica Acta 60, 2276–2765.

Lorah, M.M., Herman, J.S., 1988. The chemical evolution of a travertine-depositing stream: geochemical processes and mass transfer reactions. Water Resources Research 24, 1541–1552.

Liu, Z., Svensson, U., Dreybrodt, W., Yuan, D.X., Buhmann, D., 1995. Hydrodynamic control of inorganic calcite precipitation in Huanglong Ravine, China: field measurements and theoretical prediction of deposition rates. Geochimica et Cosmochimica Acta 59, 3087–3097.

Lu, G., Zheng, C., Donahoe, R.J., Lyons, W.B., 2000. Controlling processes in a $CaCO_3$ precipitating stream in Huanglong Natural Scenic District, Sichuan, China. Journal of Hydrology 230, 34–54.

Merz-Preiß, M., Riding, R., 1999. Cyanobacterial tufa calcification In two freshwater streams: ambient environment, chemical thresholds and biological processes. Sedimentary Geology 126, 103–124.

Pedley, H.M., 1992. Freshwater (phytoherm) reefs: the role of biofilms and their bearing on marine reef cementation. Sedimentary Geology 79, 255–274.

Pentecost, A., Lord, T., 1988. Postglacial tufas and travertines from the Craven District of Yorkshire. Cave Science 15, 15–19.

Reddy, M.M., 1977. Crystallization of calcium carbonate in presence of trace concentration of phosphorus-contained anions: I. Inhibition of phosphate and glycerophorus ions at pH 8.8 and 25 °C. Journal of Crystal Growth 41, 287–295.

Stumm, W., 1985. Chemical Processes in Lakes. Wiley, New York.

Suarez, D.L., 1983. Calcite supersaturation and precipitation kinetics in the lower Colorado River, All-American Canal, and East Highland Canal. Water Resource Research 19, 653–661.

Viles, H.A., Goudie, A.S., 1990. Tufas, travertines and allied carbonate deposits. Progress in Physical Geography 14, 19–41.

Zhang, Y., Mo, Z., 1982. The origin and evolution of Orange Fall. Acta Geographica Sinica 37, 303–316.

Zhang, D., Zhang, Y., Zhu, A., Chen, X., 2001. Physical mechanisms of river waterfall tufa (travertine) formation. Journal of Sedimentary Research 71, 205–216.